Improvement of transient performance in tracking control for discrete-time systems with input saturation and disturbances

K. Peng, G. Cheng, B.M. Chen and T.H. Lee

Abstract: The authors present an enhanced composite nonlinear feedback (CNF) control technique for discrete-time systems with input saturation and with external disturbances. The conventional CNF control is proven to be capable of yielding better transient performance in tracking control for systems with input saturation. However, when the given system has external disturbances as in most practical situations, the conventional CNF control yields some steady-state errors in the resulting output response. The enhanced CNF technique presented is an extension of the conventional one. It retains the good transient properties of the conventional CNF control and at the same time has the additional capacity for eliminating steady-state bias because of unknown constant disturbances. A numerical example and practical disk drive servo system design are provided to demonstrate the effectiveness of this control technique. Experimental results show that the new design yields a huge improvement over classical approaches.

1 Introduction

Transient performance is one of the important issues in tracking control problems that include target-tracking and output regulation (see e.g. [1, 2]). In general, quick response and a small overshoot are desirable in most of the target-tracking control problems. However, it is well-known that quick response will result in a large overshoot. Thus, most design schemes have to make a trade-off between these two transient performance indices. In this article, we have considered a tracking problem for a class of discrete-time systems with input saturation and with external disturbances. Particular attention was paid to improving the transient performance of the closed-loop system by using the so-called enhanced composite nonlinear feedback (CNF) control technique.

To improve tracking performance, Lin *et al.* [3] proposed the CNF control technique in their pioneering work on a class of second-order linear systems. Turner *et al.* [4] later extended the results of Lin *et al.* [3] to higher-order and multiple-input systems under a restrictive assumption on the system. However, both Lin *et al.* [3] and Turner *et al.* [4] only considered the state feedback case. Recently, Chen *et al.* [5] developed a CNF control to a more general class of systems with measurement feedback and successfully applied the technique to solve a hard disk drive servo problem. The discrete-time counterpart of such a technique was reported in Venkataramanan *et al.* [6].

The CNF control consists of a linear feedback law and a nonlinear feedback law without any switching element. The linear feedback part is designed to yield a closed-loop system with a small damping ratio for a quick response, whereas at the same time not exceeding the actuator limits for desired command input levels. The nonlinear feedback law is used to increase the damping ratio of the closed-loop system as the system output approaches the target reference to reduce the overshoot caused by the linear part. Basically, the CNF control design philosophy is to combine the good properties associated with larger- and smaller-damped systems.

All the above-mentioned results are not capable of tackling systems with external disturbances. In a recent work [7], an enhanced CNF technique that involved augmenting an integrator to the control system design was proposed for solving the tracking control problem for continuous-time systems with external disturbances. The enhanced procedure has proved to be capable of removing steady-state bias due to constant disturbances. This article is a counterpart to the one of Peng *et al.* [7], tackling a similar problem for discrete-time systems and is a natural extension of the conventional CNF design for discrete-time systems reported in Venkataramanan *et al.* [6]. The proposed technique has been applied to the design of a servo system for a micro hard disk drive. The design has been successfully implemented onto the actual hardware.

2 Enhanced CNF control

We considered a linear discrete-time system with actuator saturation and disturbances characterised by

$$\begin{aligned} x(k+1) &= \boldsymbol{A}x(k) + \boldsymbol{B}\,\mathrm{sat}(u(k)) + \boldsymbol{E}w, \quad x(0) = x_0 \\ y(k) &= \boldsymbol{C}_1 x(k) \\ h(k) &= \boldsymbol{C}_2 x(k) \end{aligned} \tag{1}$$

where $x \in \mathbb{R}^n$, $u \in \mathbb{R}$, $y \in \mathbb{R}^p$, $h \in \mathbb{R}$ and $w \in \mathbb{R}$ are, respectively, the state, control input, measurement output,

doi:10.1049/iet-cta:20050205

Paper first received 26th May and in revised form 31st December 2005

The authors are with the Department of Electrical and Computer Engineering, National University of Singapore, Singapore 117576

E-mail: bmchen@nus.edu.sg

controlled output and disturbance input of the system. $\boldsymbol{A}$, $\boldsymbol{B}$, $\boldsymbol{C}_1$, $\boldsymbol{C}_2$ and $\boldsymbol{E}$ are appropriate dimensional constant matrices. The function sat: $\mathbb{R} \to \mathbb{R}$ represents the actuator saturation defined as

$$\text{sat}(u(k)) = \text{sgn}(u(k)) \min\{u_{\max}, |u(k)|\} \tag{2}$$

with $u_{\max}$ being the input saturation level. The following assumptions on the given system can be made:

1. $(\boldsymbol{A}, \boldsymbol{B})$ is stabilisable;
2. $(\boldsymbol{A}, \boldsymbol{C}_1)$ is detectable;
3. $(\boldsymbol{A}, \boldsymbol{B}, \boldsymbol{C}_2)$ is invertible and has no invariant zero at $z = 1$;
4. w is bounded unknown constant disturbance; and finally,
5. $h(k)$ is a subset of $y(k)$, this is $h(k)$ is also measurable.

Note that all these assumptions are fairly standard for tracking control.

It was our aim to design a discrete enhanced CNF control law for the system with input saturation and disturbances to track a step reference, say r, neither violating the input saturation nor having steady state bias. An equivalent discrete integration, which eventually becomes part of the final control law, is defined as follows

$$x_{\mathrm{i}}(k+1) = x_{\mathrm{i}}(k) + \kappa_{\mathrm{i}} e(k) = x_{\mathrm{i}}(k) + \kappa_{\mathrm{i}} \boldsymbol{C}_2 x(k) - \kappa_{\mathrm{i}} r \tag{3}$$

where the tracking error $e(k) := h(k) - r$ is available for feedback as $h(k)$ is assumed to be measurable and κ_{i} is a positive scalar to be selected to yield an appropriate integration speed. By integrating (3) into the given system, we obtained the following augmented system

$$\begin{aligned} \bar{x}(k+1) &= \bar{\boldsymbol{A}}\bar{x}(k) + \bar{\boldsymbol{B}}\,\text{sat}(u(k)) + \bar{\boldsymbol{B}}_r r + \bar{\boldsymbol{E}} w \\ \bar{y}(k) &= \bar{\boldsymbol{C}}_1 \bar{x}(k) \\ h(k) &= \bar{\boldsymbol{C}}_2 \bar{x}(k) \end{aligned} \tag{4}$$

where

$$\bar{x}(k) = \begin{pmatrix} x_{\mathrm{i}}(k) \\ x(k) \end{pmatrix}, \quad \bar{x}_0 = \begin{pmatrix} 0 \\ x_0 \end{pmatrix}, \quad \bar{y}(k) = \begin{pmatrix} x_{\mathrm{i}}(k) \\ y(k) \end{pmatrix} \tag{5}$$

$$\bar{\boldsymbol{A}} = \begin{bmatrix} 1 & \kappa_{\mathrm{i}} C_2 \\ 0 & \boldsymbol{A} \end{bmatrix}, \quad \bar{\boldsymbol{B}} = \begin{bmatrix} 0 \\ \boldsymbol{B} \end{bmatrix}, \quad \bar{\boldsymbol{B}}_r = \begin{bmatrix} -\kappa_{\mathrm{i}} \\ 0 \end{bmatrix} \tag{6}$$

and

$$\bar{\boldsymbol{E}} = \begin{bmatrix} 0 \\ \boldsymbol{E} \end{bmatrix}, \quad \bar{\boldsymbol{C}}_1 = \begin{bmatrix} 1 & 0 \\ 0 & \boldsymbol{C}_1 \end{bmatrix}, \quad \bar{\boldsymbol{C}}_2 = [0 \quad \boldsymbol{C}_2] \tag{7}$$

Note that under Assumptions 1 and 3, it is straightforward to verify that the pair $(\bar{\boldsymbol{A}}, \bar{\boldsymbol{B}})$ is stabilisable.

An account of the design of the enhanced CNF control laws for the given system now follows for two different cases – the state feedback case and the reduced-order measurement feedback case. The full-order measurement feedback case can be solved in a straightforward manner once the result for the reduced-order case is established.

2.1 State feedback case

Consider the situation when all the state variables of the given system (1) are measurable, that is, $y = x$. The procedure that generates an enhanced CNF state feedback law can be completed in three steps. In the first step, a linear feedback control law with appropriate properties is designed and in the second step, the design of a nonlinear feedback portion will be carried out. Finally, in the last step, the linear and nonlinear feedback laws are combined to form an enhanced CNF control law.

Step 1. To design a linear feedback control law:

$$u_{\mathrm{L}}(k) = \boldsymbol{F}\bar{x}(k) + \boldsymbol{G}r \tag{8}$$

where $\boldsymbol{F}$ is chosen such that: (i) $\bar{\boldsymbol{A}} + \bar{\boldsymbol{B}}\boldsymbol{F}$ is asymptotically stable; and (ii) the closed-loop system $\bar{\boldsymbol{C}}_2(z\boldsymbol{I} - \bar{\boldsymbol{A}} - \bar{\boldsymbol{B}}\boldsymbol{F})^{-1}\bar{\boldsymbol{B}}$ has certain desired properties. $\boldsymbol{F} = [F_{\mathrm{s}} \ F_x]$ is partitioned in conformity with $x_{\mathrm{i}}(k)$ and $x(k)$. A general guideline in designing such a state feedback gain $\boldsymbol{F}$ is to place the closed-loop pole of $\bar{\boldsymbol{A}} + \bar{\boldsymbol{B}}\boldsymbol{F}$ corresponding to $x_{\mathrm{i}}(k)$ to be sufficiently closer to $z = 1$ when compared with the other eigenvalues, which implies that F_{s} is a relatively small scalar. The remaining closed-loop poles of $\bar{\boldsymbol{A}} + \bar{\boldsymbol{B}}\boldsymbol{F}$ should be placed to have a dominating pair with a small damping ratio, which in turn yields a fast rise time in the closed-loop system response. Finally, $\boldsymbol{G}$ is chosen as

$$\boldsymbol{G} = [\boldsymbol{C}_2(\boldsymbol{I} - \boldsymbol{A} - \boldsymbol{B}F_{\mathrm{x}})^{-1}\boldsymbol{B}]^{-1} \tag{9}$$

which is well defined as $(\boldsymbol{A}, \boldsymbol{B}, \boldsymbol{C}_2)$ is assumed to have no invariant zeros at $z = 1$ and $\boldsymbol{I} - \boldsymbol{A} - \boldsymbol{B}F_{\mathrm{x}}$ is non-singular whenever $\bar{\boldsymbol{A}} + \bar{\boldsymbol{B}}\boldsymbol{F}$ is stable and F_{s} is relatively small.

Step 2. Given an appropriate positive definite constant matrix, $\boldsymbol{W} \in \mathbb{R}^{(n+1)\times(n+1)}$, the following Lyapunov equation

$$\boldsymbol{P} = (\bar{\boldsymbol{A}} + \bar{\boldsymbol{B}}\boldsymbol{F})'\boldsymbol{P}(\bar{\boldsymbol{A}} + \bar{\boldsymbol{B}}\boldsymbol{F}) + \boldsymbol{W} \tag{10}$$

is solved for $\boldsymbol{P} > 0$. Such a solution is always existent as $\bar{\boldsymbol{A}} + \bar{\boldsymbol{B}}\boldsymbol{F}$ is asymptotically stable. Next, we define

$$\boldsymbol{G}_{\mathrm{e}} := \begin{bmatrix} 0 \\ (\boldsymbol{I} - \boldsymbol{A} - \boldsymbol{B}F_{\mathrm{x}})^{-1}\boldsymbol{B}\boldsymbol{G} \end{bmatrix}, \quad \bar{x}_{\mathrm{e}} := \boldsymbol{G}_{\mathrm{e}} r \tag{11}$$

The nonlinear feedback portion of the enhanced CNF control law, $u_{\mathrm{N}}(k)$, is then given by

$$u_{\mathrm{N}}(k) = \boldsymbol{\rho}(e(k))\bar{\boldsymbol{B}}'\boldsymbol{P}(\bar{\boldsymbol{A}} + \bar{\boldsymbol{B}}\boldsymbol{F})[\bar{x}(k) - \bar{x}_{\mathrm{e}}] \tag{12}$$

where $\boldsymbol{\rho}(e(k))$, with $e = h - r$, is a non-positive function of $|e|$ and tends to a finite scalar as $k \to \infty$. It is used to gradually change the system closed-loop damping ratio to yield a better tracking performance. The choice of the design parameters, $\boldsymbol{\rho}(e(k))$ and $\boldsymbol{W}$, will be discussed later.

Step 3. The linear and nonlinear feedback control laws derived in the previous steps are now combined to form an enhanced CNF control law

$$u(k) = \boldsymbol{F}\bar{x}(k) + \boldsymbol{G}r + \boldsymbol{\rho}(e(k))\bar{\boldsymbol{B}}'\boldsymbol{P}(\bar{\boldsymbol{A}} + \bar{\boldsymbol{B}}\boldsymbol{F})[\bar{x}(k) - \bar{x}_{\mathrm{e}}] \tag{13}$$

Thus, we have the following result.

Theorem 1: Consider the given system (1) with $y = x$ and the disturbance w bounded by a non-negative scalar τ_w, that is, $|w| \le \tau_w$. Let

$$\gamma := [1 - (1 - \lambda_{\min}(\boldsymbol{W}\boldsymbol{P}^{-1}))^{1/2}]^{-1}(\bar{\boldsymbol{E}}'\boldsymbol{P}\bar{\boldsymbol{E}})^{1/2}\tau_w \tag{14}$$

Then, for any $\boldsymbol{\rho}(e(k)) \in [-2(\bar{\boldsymbol{B}}'\boldsymbol{P}\bar{\boldsymbol{B}})^{-1}, 0]$, which is a non-positive function of $|e|$ and tends to a constant, $\boldsymbol{\rho}_\infty$, as $k \to \infty$, the enhanced CNF control law (13) will drive the system controlled output $h(k)$ to track the step reference of amplitude r from an initial state $\bar{x}_0$ asymptotically without steady-state error, provided that the following conditions are satisfied:

1. There exist scalars $\delta \in (0, 1)$, $c_\delta > \gamma^2$ and $c_\rho > \gamma^2$ such that

$$\forall \bar{x}(k) \in \boldsymbol{X}(\boldsymbol{F}, c_\delta) := \{\bar{x}(k): \bar{x}'(k)\boldsymbol{P}\bar{x}(k) \le c_\delta\} \Rightarrow |\boldsymbol{F}\bar{x}(k)| \le (1-\delta)u_{\max} \quad (15)$$

and

$$\forall \bar{x}(k) \in \boldsymbol{X}(\boldsymbol{F}, \boldsymbol{P}, c_\rho) := \{\bar{x}(k): \bar{x}'(k)\boldsymbol{P}\bar{x}(k) \le c_\rho\} \Rightarrow |(\boldsymbol{F} + \boldsymbol{\rho}_\infty \bar{\boldsymbol{B}}'\boldsymbol{P}(\bar{\boldsymbol{A}} + \bar{\boldsymbol{B}}\boldsymbol{F}))\bar{x}(k)| \le (1-\delta)u_{\max} \quad (16)$$

Note that (16) implies that the control signal does not exceed the saturation level in the face of disturbances when the controlled output approaches the target.

2. The initial condition, $\bar{x}_0$, satisfies

$$\bar{x}_0 - \bar{x}_{\mathrm{e}} \in \boldsymbol{X}(\boldsymbol{F}, c_\delta) \quad (17)$$

3. The level of the target reference, r, satisfies

$$|Hr| \le \delta u_{\max} \quad (18)$$

where $H := \boldsymbol{F}\boldsymbol{G}_{\mathrm{e}} + \boldsymbol{G}$. Note that $\lambda_{\min}(\boldsymbol{W}\boldsymbol{P}^{-1}) \in (0, 1)$.

Proof: For simplicity, we will drop $e(k)$ in the nonlinear function $\boldsymbol{\rho}$ throughout the following proof. First of all, it is straightforward to verify that

$$\bar{\boldsymbol{A}}\bar{x}_{\mathrm{e}} + \bar{\boldsymbol{B}}\boldsymbol{H}r + \bar{\boldsymbol{B}}_{\mathrm{r}}r = \bar{x}_{\mathrm{e}} \quad (19)$$

Letting $\tilde{x}(k) = \bar{x}(k) - \bar{x}_{\mathrm{e}}$, the augmented system (4) can be expressed as

$$\tilde{x}(k+1) = (\bar{\boldsymbol{A}} + \bar{\boldsymbol{B}}\boldsymbol{F})\tilde{x}(k) + \bar{\boldsymbol{B}}v(k) + \bar{\boldsymbol{E}}w \quad (20)$$

where

$$v(k) := \mathrm{sat}(u(k)) - \boldsymbol{F}\tilde{x}(k) - \boldsymbol{H}r \quad (21)$$

and the control law (13) can be rewritten as

$$u(k) = \boldsymbol{F}\tilde{x}(k) + \boldsymbol{H}r + \boldsymbol{\rho}\bar{\boldsymbol{B}}'\boldsymbol{P}(\bar{\boldsymbol{A}} + \bar{\boldsymbol{B}}\boldsymbol{F})\tilde{x}(k) \quad (22)$$

Next, for $\tilde{x}(k) \in \boldsymbol{X}(\boldsymbol{F}, c_\delta)$ and $|\boldsymbol{H}r| \le \delta u_{\max}$, we have

$$|\boldsymbol{F}\tilde{x}(k) + \boldsymbol{H}r| \le |\boldsymbol{F}\tilde{x}(k)| + |\boldsymbol{H}r| \le u_{\max} \quad (23)$$

which implies

$$v(k) = \boldsymbol{\rho}\bar{\boldsymbol{B}}'\boldsymbol{P}(\bar{\boldsymbol{A}} + \bar{\boldsymbol{B}}\boldsymbol{F})\tilde{x}(k) \quad (24)$$

if $|u(k)| \le u_{\max}$, or

$$0 < v(k) < \boldsymbol{\rho}\bar{\boldsymbol{B}}'\boldsymbol{P}(\bar{\boldsymbol{A}} + \bar{\boldsymbol{B}}\boldsymbol{F})\tilde{x}(k) \quad (25)$$

if $u(k) > u_{\max}$, or

$$\boldsymbol{\rho}\bar{\boldsymbol{B}}'\boldsymbol{P}(\bar{\boldsymbol{A}} + \bar{\boldsymbol{B}}\boldsymbol{F})\tilde{x}(k) < v(k) < 0 \quad (26)$$

if $u(k) < -u_{\max}$. Obviously, for all possible situations, $v(k)$ can be written as

$$v(k) = \boldsymbol{q}\boldsymbol{\rho}\bar{\boldsymbol{B}}'\boldsymbol{P}(\bar{\boldsymbol{A}} + \bar{\boldsymbol{B}}\boldsymbol{F})\tilde{x}(k) \quad (27)$$

with some appropriate $\boldsymbol{q} \in [0, 1]$. Thus, for $\tilde{x}(k) \in \boldsymbol{X}(\boldsymbol{F}, c_\delta)$ and $|\boldsymbol{H}r| \le \delta u_{\max}$, the closed-loop system comprising the augmented system (4) and the CNF control law (13) can be expressed as follows

$$\tilde{x}(k+1) = [\bar{\boldsymbol{A}} + \bar{\boldsymbol{B}}\boldsymbol{F} + \boldsymbol{q}\boldsymbol{\rho}\bar{\boldsymbol{B}}\bar{\boldsymbol{B}}'\boldsymbol{P}(\bar{\boldsymbol{A}} + \bar{\boldsymbol{B}}\boldsymbol{F})]\tilde{x}(k) + \bar{\boldsymbol{E}}w \quad (28)$$

Defining a Lyapunov function, $\boldsymbol{V}(k) = \tilde{x}'(k)\boldsymbol{P}\tilde{x}(k)$, and factoring $\boldsymbol{P} > 0$ as $\boldsymbol{P} = \boldsymbol{S}'\boldsymbol{S}$, the increment of $V(k)$ along the trajectory of the system (28) can be calculated as

$$\begin{aligned}\Delta\boldsymbol{V}(k) &= -\tilde{x}'(k)\boldsymbol{P}\tilde{x}(k) + \tilde{x}'(k)(\bar{\boldsymbol{A}} + \bar{\boldsymbol{B}}\boldsymbol{F})'\boldsymbol{P}(\bar{\boldsymbol{A}} + \bar{\boldsymbol{B}}\boldsymbol{F})\tilde{x}(k)\\ &\quad + \tilde{x}'(k)(\bar{\boldsymbol{A}} + \bar{\boldsymbol{B}}\boldsymbol{F})'\boldsymbol{P}\bar{\boldsymbol{B}}(2\boldsymbol{q}\boldsymbol{\rho} + \boldsymbol{q}^2\boldsymbol{\rho}^2\bar{\boldsymbol{B}}'\boldsymbol{P}\bar{\boldsymbol{B}})\\ &\quad \times \bar{\boldsymbol{B}}'\boldsymbol{P}(\bar{\boldsymbol{A}} + \bar{\boldsymbol{B}}\boldsymbol{F})\tilde{x}(k) + w'\bar{\boldsymbol{E}}'\boldsymbol{P}\bar{\boldsymbol{E}}w\\ &\quad + 2\tilde{x}'(k)(\bar{\boldsymbol{A}} + \bar{\boldsymbol{B}}\boldsymbol{F})'(\boldsymbol{I} + \boldsymbol{q}\boldsymbol{\rho}\bar{\boldsymbol{B}}\bar{\boldsymbol{B}}'\boldsymbol{P})'\boldsymbol{P}\bar{\boldsymbol{E}}w\\ &\le -\tilde{x}'(k)\boldsymbol{P}\tilde{x}(k) + \tilde{x}'(k)(\boldsymbol{P} - \boldsymbol{W})\tilde{x}(k) + \bar{\boldsymbol{E}}'\boldsymbol{P}\bar{\boldsymbol{E}}\tau_w^2\\ &\quad + 2\|\tilde{x}'(k)(\bar{\boldsymbol{A}} + \bar{\boldsymbol{B}}\boldsymbol{F})'(\boldsymbol{I} + \boldsymbol{q}\boldsymbol{\rho}\bar{\boldsymbol{B}}\bar{\boldsymbol{B}}'\boldsymbol{P})'\boldsymbol{S}'\| \times \|\boldsymbol{S}\bar{\boldsymbol{E}}\|\tau_w\end{aligned}$$

Noting that

$$\begin{aligned}&\|\tilde{x}'(k)(\bar{\boldsymbol{A}} + \bar{\boldsymbol{B}}\boldsymbol{F})'(\boldsymbol{I} + \boldsymbol{q}\boldsymbol{\rho}\bar{\boldsymbol{B}}\bar{\boldsymbol{B}}'\boldsymbol{P})'\boldsymbol{S}'\|\\ &\quad \le [\tilde{x}'(k)(\bar{\boldsymbol{A}} + \bar{\boldsymbol{B}}\boldsymbol{F})'\boldsymbol{P}(\bar{\boldsymbol{A}} + \bar{\boldsymbol{B}}\boldsymbol{F})\tilde{x}(k)]^{1/2}\end{aligned} \quad (29)$$

for $\boldsymbol{\rho} \in [-2(\bar{\boldsymbol{B}}'\boldsymbol{P}\bar{\boldsymbol{B}})^{-1}, 0]$, we have

$$\begin{aligned}\Delta\boldsymbol{V}(k) &\le -\tilde{x}'(k)\boldsymbol{P}\tilde{x}(k) + \tilde{x}'(k)(\boldsymbol{P} - \boldsymbol{W})\tilde{x}(k) + \bar{\boldsymbol{E}}'\boldsymbol{P}\bar{\boldsymbol{E}}\tau_w^2\\ &\quad + 2[\tilde{x}'(k)(\bar{\boldsymbol{A}} + \bar{\boldsymbol{B}}\boldsymbol{F})'\boldsymbol{P}(\bar{\boldsymbol{A}} + \bar{\boldsymbol{B}}\boldsymbol{F})\tilde{x}(k)]^{1/2}(\bar{\boldsymbol{E}}'\boldsymbol{P}\bar{\boldsymbol{E}})^{1/2}\tau_w\\ &= -\big\{(\tilde{x}'(k)\boldsymbol{P}\tilde{x}(k))^{1/2} + [\tilde{x}'(k)(\boldsymbol{P} - \boldsymbol{W})\tilde{x}(k)]^{1/2}\\ &\quad + (\bar{\boldsymbol{E}}'\boldsymbol{P}\bar{\boldsymbol{E}})^{1/2}\tau_w\big\}\big\{(\tilde{x}'(k)\boldsymbol{P}\tilde{x}(k))^{1/2}\\ &\quad - [\tilde{x}'(k)(\boldsymbol{P} - \boldsymbol{W})\tilde{x}(k)]^{1/2} - (\bar{\boldsymbol{E}}'\boldsymbol{P}\bar{\boldsymbol{E}})^{1/2}\tau_w\big\}\\ &= -\big\{(\tilde{x}'(k)\boldsymbol{P}\tilde{x}(k))^{1/2} + [\tilde{x}'(k)(\boldsymbol{P} - \boldsymbol{W})\tilde{x}(k)]^{1/2}\\ &\quad + (\bar{\boldsymbol{E}}'\boldsymbol{P}\bar{\boldsymbol{E}})^{1/2}\tau_w\big\}\Bigg\{ - (\bar{\boldsymbol{E}}'\boldsymbol{P}\bar{\boldsymbol{E}})^{1/2}\tau_w + (\tilde{x}'(k)\boldsymbol{P}\tilde{x}(k))^{1/2}\\ &\quad \times \left[1 - \left(1 - \frac{\tilde{x}'(k)\boldsymbol{W}\tilde{x}(k)}{\tilde{x}'(k)\boldsymbol{P}\tilde{x}(k)}\right)^{1/2}\right]\Bigg\}\\ &\le -\big\{(\tilde{x}'(k)\boldsymbol{P}\tilde{x}(k))^{1/2} + [\tilde{x}'(k)(\boldsymbol{P} - \boldsymbol{W})\tilde{x}(k)]^{1/2}\\ &\quad + (\bar{\boldsymbol{E}}'\boldsymbol{P}\bar{\boldsymbol{E}})^{1/2}\tau_w\big\} \times \big\{-(\bar{\boldsymbol{E}}'\boldsymbol{P}\bar{\boldsymbol{E}})^{1/2}\tau_w\\ &\quad + (\tilde{x}'(k)\boldsymbol{P}\tilde{x}(k))^{1/2}\big[1 - (1 - \lambda_{\min}(\boldsymbol{W}\boldsymbol{P}^{-1}))^{1/2}\big]\big\}\\ &= -\big\{(\tilde{x}'(k)\boldsymbol{P}\tilde{x}(k))^{1/2} + \big[\tilde{x}'(k)(\boldsymbol{P} - \boldsymbol{W})\tilde{x}(k)\big]^{1/2}\\ &\quad + (\bar{\boldsymbol{E}}'\boldsymbol{P}\bar{\boldsymbol{E}})^{1/2}\tau_w\big\}\big[1 - (1 - \lambda_{\min}(\boldsymbol{W}\boldsymbol{P}^{-1}))^{1/2}\big]\\ &\quad \times [(\tilde{x}'(k)\boldsymbol{P}\tilde{x}(k))^{1/2} - \gamma]\end{aligned}$$

Note that we have used the following properties

$$\lambda_{\min}(\boldsymbol{W}\boldsymbol{P}^{-1}) = \min_{x \ne 0}\frac{x'\boldsymbol{W}x}{x'\boldsymbol{P}x} \quad (30)$$

as both $\boldsymbol{W}$ and $\boldsymbol{P}$ are positive definite matrices. Clearly, the closed-loop system in the absence of the disturbance, w, has $\Delta\boldsymbol{V}(k) < 0$ and thus is asymptotically stable.

With the presence of the disturbance, w, and with $\tilde{x}(0) = \bar{x}_0 - \bar{x}_{\mathrm{e}} \in \boldsymbol{X}(\boldsymbol{F}, c_\delta)$, where $c_\delta > \gamma^2$, the corresponding trajectory of (28) will remain in $\boldsymbol{X}(\boldsymbol{F}, c_\delta)$ and converge to a ball characterised by $\{\tilde{x}: \tilde{x}'\boldsymbol{P}\tilde{x} \le \tilde{\gamma}^2\}$ with $\tilde{\gamma} \le \gamma$.

Note that $\boldsymbol{\rho}$ is chosen such that it tends to a constant as $k \to \infty$. Also, for large k, the control signal $u(k)$ will be under its saturation level because of the second portion of condition 1. Thus, the closed-loop system (28) becomes an almost linear time-invariant system. We concluded that the corresponding trajectory of (28) converged asymptotically to a point; that is, $\tilde{x}(k)$ will tend to a constant. Thus

$$\lim_{k\to\infty} e(k) = \lim_{k\to\infty} \frac{1}{\kappa_i}[x_i(k+1) - x_i(k)] = 0 \tag{31}$$

This completes the proof of Theorem 1 □

2.2 Measurement feedback case

Next, we consider the general measurement feedback situation, in which there is only part of the state variables available for feedback. As usual, for such a situation, one could either design a full-order or a reduced-order measurement feedback control law. In this article, we focused on designing a reduced-order controller. Without loss of generality, we assumed that $\boldsymbol{C}_1$ in the measurement output of the given plant (1) is in the form: $\boldsymbol{C}_1 = [\boldsymbol{I}_p\ 0]$. The augmented plant (4) can then be partitioned as

$$\begin{pmatrix} x_i \\ x_1 \\ x_2 \end{pmatrix}(k+1) = \begin{bmatrix} 1 & \kappa_i \boldsymbol{C}_{21} & \kappa_i \boldsymbol{C}_{22} \\ 0 & \boldsymbol{A}_{11} & \boldsymbol{A}_{12} \\ 0 & \boldsymbol{A}_{21} & \boldsymbol{A}_{22} \end{bmatrix} \begin{pmatrix} x_i \\ x_1 \\ x_2 \end{pmatrix}(k) + \begin{bmatrix} 0 \\ \boldsymbol{B}_1 \\ \boldsymbol{B}_2 \end{bmatrix} \mathrm{sat}(u(k)) + \begin{bmatrix} -\kappa_i \\ 0 \\ 0 \end{bmatrix} r + \begin{bmatrix} 0 \\ \boldsymbol{E}_1 \\ \boldsymbol{E}_2 \end{bmatrix} w \tag{32}$$

$$\bar{y}(k) = \begin{bmatrix} 1 & 0 & 0 \\ 0 & \boldsymbol{I}_p & 0 \end{bmatrix} \begin{pmatrix} x_i \\ x_1 \\ x_2 \end{pmatrix}(k) \tag{33}$$

and

$$h(k) = [\,0 \quad \boldsymbol{C}_{21} \quad \boldsymbol{C}_{22}\,] \begin{pmatrix} x_i \\ x_1 \\ x_2 \end{pmatrix}(k) \tag{34}$$

with

$$\begin{pmatrix} x_i(0) \\ x_1(0) \\ x_2(0) \end{pmatrix} = \begin{pmatrix} 0 \\ x_{10} \\ x_{20} \end{pmatrix} = \bar{x}_0 \tag{35}$$

We only need to estimate $x_2(k)$. There are two main steps in designing a reduced-order measurement feedback control law: (i) the construction of a full state feedback gain matrix $\boldsymbol{F}$, which is identical to that given in the previous subsection; and (ii) design of the reduced-order observer gain matrix $\boldsymbol{K}_R$, such that the poles of $\boldsymbol{A}_{22} + \boldsymbol{K}_R\boldsymbol{A}_{12}$ are placed at appropriate locations inside the unit circle. Next, given a positive definite matrix $\boldsymbol{W} \in \mathbb{R}^{(n+1)\times(n+1)}$, let $\boldsymbol{P} > 0$ be the solution to the Lyapunov equation

$$\boldsymbol{P} = (\bar{\boldsymbol{A}} + \bar{\boldsymbol{B}}\boldsymbol{F})'\boldsymbol{P}(\bar{\boldsymbol{A}} + \bar{\boldsymbol{B}}\boldsymbol{F}) + \boldsymbol{W} \tag{36}$$

The reduced-order enhanced CNF control law is then obtained by

$$\begin{aligned} x_v(k+1) &= (\boldsymbol{A}_{22} + \boldsymbol{K}_R\boldsymbol{A}_{12})x_v(k) + (\boldsymbol{B}_2 + \boldsymbol{K}_R\boldsymbol{B}_1)\,\mathrm{sat}(u(k)) \\ &\quad + [\boldsymbol{A}_{21} + \boldsymbol{K}_R\boldsymbol{A}_{11} - (\boldsymbol{A}_{22} + \boldsymbol{K}_R\boldsymbol{A}_{12})\boldsymbol{K}_R]\,y(k) \end{aligned} \tag{37}$$

and

$$u(k) = \boldsymbol{F}x_r(k) + \boldsymbol{G}r + \boldsymbol{\rho}(e(k))\bar{\boldsymbol{B}}'\boldsymbol{P}(\bar{\boldsymbol{A}} + \bar{\boldsymbol{B}}\boldsymbol{F})[x_r(k) - \bar{x}_e] \tag{38}$$

where

$$x_r(k) = \begin{pmatrix} x_i(k) \\ x_1(k) \\ x_v(k) - \boldsymbol{K}_R y(k) \end{pmatrix}$$

$\boldsymbol{G}$ is as defined in (9), $\bar{x}_e$ is as defined in (11) and $\boldsymbol{\rho}(e(k))$ is the non-positive function of $|e(k)|$, which tends to a constant as $k \to \infty$.

Next, $\boldsymbol{F} = [\boldsymbol{F}_i\ \boldsymbol{F}_1\ \boldsymbol{F}_2]$ is partitioned in conformity with $x_i(k)$, $x_1(k)$ and $x_2(k)$. Let $\boldsymbol{W}_R \in \mathbb{R}^{(n-p)\times(n-p)}$ be a positive definite matrix such that

$$\boldsymbol{W}_R > \boldsymbol{F}_2'[\bar{\boldsymbol{B}}'\boldsymbol{P}\bar{\boldsymbol{B}} + \bar{\boldsymbol{B}}'\boldsymbol{P}(\bar{\boldsymbol{A}} + \bar{\boldsymbol{B}}\boldsymbol{F})\boldsymbol{W}^{-1}(\bar{\boldsymbol{A}} + \bar{\boldsymbol{B}}\boldsymbol{F})'\boldsymbol{P}\bar{\boldsymbol{B}}]\boldsymbol{F}_2 \tag{39}$$

and let $\boldsymbol{Q}_R > 0$ be the solution to the Lyapunov equation

$$\boldsymbol{Q}_R = (\boldsymbol{A}_{22} + \boldsymbol{K}_R\boldsymbol{A}_{12})'\boldsymbol{Q}_R(\boldsymbol{A}_{22} + \boldsymbol{K}_R\boldsymbol{A}_{12}) + \boldsymbol{W}_R \tag{40}$$

Note that such a $\boldsymbol{Q}_R$ exists as $\boldsymbol{A}_{22}+\boldsymbol{K}_R\boldsymbol{A}_{12}$ is asymptotically stable. Next, let

$$\lambda_R := \lambda_{\min}\left\{ \begin{bmatrix} \boldsymbol{P} & 0 \\ 0 & \boldsymbol{Q}_R \end{bmatrix}^{-1} \times \begin{bmatrix} \boldsymbol{W} & -(\bar{\boldsymbol{A}} + \bar{\boldsymbol{B}}\boldsymbol{F})'\boldsymbol{P}\bar{\boldsymbol{B}}\boldsymbol{F}_2 \\ -\boldsymbol{F}_2'\bar{\boldsymbol{B}}'\boldsymbol{P}(\bar{\boldsymbol{A}} + \bar{\boldsymbol{B}}\boldsymbol{F}) & \boldsymbol{W}_R - \boldsymbol{F}_2'\bar{\boldsymbol{B}}'\boldsymbol{P}\bar{\boldsymbol{B}}\boldsymbol{F}_2 \end{bmatrix} \right\} \tag{41}$$

It is noted that $\lambda_R \in (0, 1)$. We have the following result.

Theorem 2: Consider the given system (1) with the disturbance w being bounded by a scalar $\tau_w > 0$, that is, $|w| \le \tau_w$. Let

$$\gamma_R := [1 - (1 - \lambda_R)^{1/2}]^{-1}[\bar{\boldsymbol{E}}'\boldsymbol{P}\bar{\boldsymbol{E}} + (\boldsymbol{E}_2 + \boldsymbol{K}_R\boldsymbol{E}_1)' \times \boldsymbol{Q}_R(\boldsymbol{E}_2 + \boldsymbol{K}_R\boldsymbol{E}_1)]^{1/2}\tau_w \tag{42}$$

Then, there exists a $\boldsymbol{\rho}^* \in (0, 2(\bar{\boldsymbol{B}}'\boldsymbol{P}\bar{\boldsymbol{B}})^{-1}]$ such that for any $\boldsymbol{\rho}(e(k)) \in [-\boldsymbol{\rho}^*, 0]$, which is a non-positive function of $|e(k)|$ and tends to a constant, $\boldsymbol{\rho}_\infty$, as $k \to \infty$, the reduced-order enhanced CNF control law of (37) and (38) will drive the system controlled output $h(k)$ to track the step reference of amplitude r asymptotically without steady-state error, provided that the following conditions are satisfied:

1. There exist positive scalars $\delta \in (0, 1)$, $c_{R\delta} > \gamma_R^2$ and $c_{R\rho} > \gamma_R^2$ such that

$$\forall \bar{x}(k) \in \boldsymbol{X}(\boldsymbol{F}, c_{R\delta}) := \left\{ \bar{x}(k):\ \bar{x}'(k)\begin{bmatrix} \boldsymbol{P} & 0 \\ 0 & \boldsymbol{Q}_R \end{bmatrix}\bar{x}(k) \le c_{R\delta} \right\} \tag{43}$$

$$\Rightarrow |[\boldsymbol{F} \quad \boldsymbol{F}_2]\bar{x}(k)| \le (1 - \delta)u_{\max} \tag{44}$$

and

$$\forall \tilde{x}(k) \in \boldsymbol{X}(\boldsymbol{F}, \boldsymbol{P}, c_{\mathrm{R}\rho}) := \left\{ \tilde{x}(k) \colon \tilde{x}'(k) \begin{bmatrix} \boldsymbol{P} & 0 \\ 0 & \boldsymbol{Q}_{\mathrm{R}} \end{bmatrix} \tilde{x}(k) \le c_{\mathrm{R}\rho} \right\} \tag{45}$$

$$\Rightarrow |[\boldsymbol{F} + \boldsymbol{\rho}_\infty \bar{\boldsymbol{B}}' \boldsymbol{P}(\bar{\boldsymbol{A}} + \bar{\boldsymbol{B}}\boldsymbol{F})\boldsymbol{F}_2 + \boldsymbol{\rho}_\infty \bar{\boldsymbol{B}}' \boldsymbol{P}(\bar{\boldsymbol{A}}_2 + \bar{\boldsymbol{B}}\boldsymbol{F}_2)]\tilde{x}(k)| \le (1-\delta)u_{\max} \tag{46}$$

where $\bar{\boldsymbol{A}}_2$ is the right hand part of matrix $\bar{\boldsymbol{A}}$ in conformity with $x_2(k)$.

2. The initial conditions, $\bar{x}_0$ and $x_{v0} = x_v(0)$, satisfy

$$\begin{pmatrix} \bar{x}_0 - \bar{x}_e \\ x_{v0} - x_{20} - K_{\mathrm{R}} x_{10} \end{pmatrix} \in \boldsymbol{X}(\boldsymbol{F}, c_{\mathrm{R}\delta}) \tag{47}$$

3. The level of the target reference, r, satisfies

$$|\boldsymbol{H}r| \le \delta u_{\max} \tag{48}$$

where $\boldsymbol{H}$ is the same as that defined in Theorem 1.

Proof: The result follows the similar lines of reasoning as given in Theorem 1 and the similar arguments for the measurement feedback case reported in Chen *et al.* [5]. □

2.3 Selection of nonlinear feedback parameters

The key component in designing the CNF controllers was the selection of $\boldsymbol{\rho}$ (hereafter, we drop the dependent variables of $\boldsymbol{\rho}$ for simplicity) and $\boldsymbol{W}$. The freedom to choose the nonlinear function $\boldsymbol{\rho}$ was used to tune the control laws so as to improve the performance of the closed-loop system, as the controlled output h approaches the set point. As the main purpose of adding the nonlinear part to the CNF controller was to speed up the settling time and to reduce the overshoot, or equivalently to contribute a significant value to the control input when the tracking error, $r - h$, was small, it was appropriate for us to select a nonlinear gain matrix such that the nonlinear part would be in action when the control signal was far away from its saturation level, and thus it would not cause the control input to hit its limits. Under such a circumstance, it was straightforward to verify that the closed-loop system comprising the augmented plant in (4) and the CNF control law (13) could be expressed as

$$\tilde{x}(k+1) = (\bar{\boldsymbol{A}} + \bar{\boldsymbol{B}}F)\tilde{x}(k) + \boldsymbol{\rho}\bar{\boldsymbol{B}}\bar{\boldsymbol{B}}'\boldsymbol{P}(\bar{\boldsymbol{A}} + \bar{\boldsymbol{B}}\boldsymbol{F})\tilde{x}(k) + \bar{\boldsymbol{E}}w \tag{49}$$

Clearly, eigenvalues of the closed-loop system in (49) can be changed by the nonlinear function $\boldsymbol{\rho}$. Assuming that h is available and assuming that $h(0) \ne r$ (for the trivial case when $h(0) = r$, there is no need to add any nonlinear gain to the control), the following nonlinear gain matrix is proposed

$$\boldsymbol{\rho}(e(k)) = -\beta(\bar{\boldsymbol{B}}'\boldsymbol{P}\bar{\boldsymbol{B}})^{-1}\frac{2}{\pi}\arctan\left(\alpha\Big||e(k)| - |h(0) - r|\Big|\right) \tag{50}$$

with $0 \le \beta \le 2$. $\boldsymbol{\rho}$ starts from 0 and decreases to a constant $-\beta(\bar{\boldsymbol{B}}'\boldsymbol{P}\bar{\boldsymbol{B}})^{-1}2\arctan(\alpha|h(0) - r|)/\pi > -\beta(\bar{\boldsymbol{B}}'\boldsymbol{P}\bar{\boldsymbol{B}})^{-1}$ as h approaches the target reference r. The parameter α is used to determine the speed of change in $\boldsymbol{\rho}$.

To examine the behaviour of the closed-loop system (49) more explicitly, we defined an auxiliary system $\boldsymbol{G}_{\mathrm{aux}}(z)$ characterised by

$$\boldsymbol{G}_{\mathrm{aux}}(z) := \boldsymbol{C}_{\mathrm{aux}}(z\boldsymbol{I} - \boldsymbol{A}_{\mathrm{aux}})^{-1}\boldsymbol{B}_{\mathrm{aux}} := \bar{\boldsymbol{B}}'\boldsymbol{P}(z\boldsymbol{I} - \bar{\boldsymbol{A}} - \bar{\boldsymbol{B}}\boldsymbol{F})^{-1}\bar{\boldsymbol{B}} \tag{51}$$

Clearly, $\boldsymbol{G}_{\mathrm{aux}}(z)$ is stable. Note that $\boldsymbol{C}_{\mathrm{aux}}\boldsymbol{B}_{\mathrm{aux}} = \bar{\boldsymbol{B}}'\boldsymbol{P}\bar{\boldsymbol{B}} > 0$, which implies $\boldsymbol{G}_{\mathrm{aux}}(z)$ is a square, invertible and uniform rank system with a relative degree of 1 and with n invariant zeros. This auxiliary system is in fact of minimum phase, that is, all its invariant zeros are stable. Note that for such a system, it follows from the result reported in Chapter 5 of Chen *et al.* [8] that there exists non-singular transformations $\Gamma_s \in \mathbb{R}^{(n+1)\times(n+1)}$, $\Gamma_i \in \mathbb{R}$ and $\Gamma_o \in \mathbb{R}$ such that the transformed system has the following special form

$$(\Gamma_s^{-1}\boldsymbol{A}_{\mathrm{aux}}\Gamma_s,\ \Gamma_s^{-1}\boldsymbol{B}_{\mathrm{aux}}\Gamma_i,\ \Gamma_o^{-1}\boldsymbol{C}_{\mathrm{aux}}\Gamma_s) = \left(\begin{bmatrix} \boldsymbol{A}_{\mathrm{aa}} & \boldsymbol{L}_{\mathrm{ad}} \\ \boldsymbol{E}_{\mathrm{da}} & \boldsymbol{A}_{\mathrm{dd}} \end{bmatrix}, \begin{bmatrix} 0 \\ 1 \end{bmatrix}, [0 \quad 1]\right) \tag{52}$$

where the eigenvalues of $\boldsymbol{A}_{\mathrm{aa}}$ are the invariant zeros of the auxiliary system, $\boldsymbol{G}_{\mathrm{aux}}(z)$, $\boldsymbol{L}_{\mathrm{ad}}$, $\boldsymbol{E}_{\mathrm{da}}$ and $\boldsymbol{A}_{\mathrm{dd}}$ are some constant matrices. Next, it can be shown that all the eigenvalues of $\boldsymbol{A}_{\mathrm{aa}}$ are inside the unit circle and thus $\boldsymbol{G}_{\mathrm{aux}}(z)$ is of minimum phase. Note that at the steady state when $h = r$, the nonlinear function $\boldsymbol{\rho}$ of (50) with an appropriately chosen β can be set to $\boldsymbol{\rho} = -(\bar{\boldsymbol{B}}'\boldsymbol{P}\bar{\boldsymbol{B}})^{-1}$ and the closed-loop system of (49) can be expressed as

$$\begin{aligned}
\tilde{x}(k+1) &= (\bar{\boldsymbol{A}} + \bar{\boldsymbol{B}}\boldsymbol{F})\tilde{x}(k) - \bar{\boldsymbol{B}}(\bar{\boldsymbol{B}}'\boldsymbol{P}\bar{\boldsymbol{B}})^{-1}\bar{\boldsymbol{B}}'\boldsymbol{P}(\bar{\boldsymbol{A}} + \bar{\boldsymbol{B}}\boldsymbol{F})\tilde{x}(k) \\
&= [\boldsymbol{I} - \bar{\boldsymbol{B}}(\bar{\boldsymbol{B}}'\boldsymbol{P}\bar{\boldsymbol{B}})^{-1}\bar{\boldsymbol{B}}'\boldsymbol{P}](\bar{\boldsymbol{A}} + \bar{\boldsymbol{B}}\boldsymbol{F})\tilde{x}(k) \\
&= [\boldsymbol{I} - \boldsymbol{B}_{\mathrm{aux}}(\boldsymbol{C}_{\mathrm{aux}}\boldsymbol{B}_{\mathrm{aux}})^{-1}\boldsymbol{C}_{\mathrm{aux}}]\boldsymbol{A}_{\mathrm{aux}}\tilde{x}(k) \\
&= \left[\boldsymbol{I} - \Gamma_s\begin{bmatrix} 0 \\ 1 \end{bmatrix}\Gamma_i^{-1}\left(\Gamma_o[0 \quad 1]\Gamma_s^{-1}\Gamma_s\begin{bmatrix} 0 \\ 1 \end{bmatrix}\Gamma_i^{-1}\right)^{-1} \times \Gamma_o[0 \quad 1]\Gamma_s^{-1}\right]\Gamma_s\begin{bmatrix} \boldsymbol{A}_{\mathrm{aa}} & \boldsymbol{L}_{\mathrm{ad}} \\ \boldsymbol{E}_{\mathrm{da}} & \boldsymbol{A}_{\mathrm{dd}} \end{bmatrix}\Gamma_s^{-1}\tilde{x}(k) \\
&= \left(\Gamma_s\begin{bmatrix} \boldsymbol{A}_{\mathrm{aa}} & \boldsymbol{L}_{\mathrm{ad}} \\ 0 & 0 \end{bmatrix}\Gamma_s^{-1}\right)\tilde{x}(k)
\end{aligned} \tag{53}$$

Clearly, the closed-loop system has n eigenvalues at $\lambda(\boldsymbol{A}_{\mathrm{aa}})$ and one at 0. Thus, the stability of the closed-loop system with $\boldsymbol{\rho} = -(\bar{\boldsymbol{B}}'\boldsymbol{P}\bar{\boldsymbol{B}})^{-1}$ implies the eigenvalues of $\boldsymbol{A}_{\mathrm{aa}}$ are all inside the unit circle. This shows that $\boldsymbol{G}_{\mathrm{aux}}(z)$ is indeed of minimum phase.

It should be noted that there is a freedom in pre-selecting the locations of these invariant zeros by choosing an appropriate $\boldsymbol{W}$ in (10). In general, invariant zeros of $\boldsymbol{G}_{\mathrm{aux}}(z)$ should be selected, which correspond to the closed-loop poles of (49) for the steady-state nonlinear gain matrix, with the dominating ones having a large damping ratio. This, in turn, generally yields a smaller overshoot. The following procedure might be used for such a purpose.

1. Given a set of n self-conjugated complex scalars, which should include all the uncontrollable modes, if any, of $(\bar{\boldsymbol{A}}, \bar{\boldsymbol{B}})$, we were able to determine an appropriate $\boldsymbol{W} > 0$ such that the resulting auxiliary system $\boldsymbol{G}_{\mathrm{aux}}(z)$ had its invariant zeros placed exactly at the locations given in the set.

First, the singular value decomposition technique was used to find a unitary matrix $\boldsymbol{U} \in \mathbb{R}^{n \times n}$ and a non-singular matrix $\boldsymbol{T}_{\mathrm{i}} \in \mathbb{R}^{m \times m}$ such that

$$\tilde{\boldsymbol{B}}_{\text{aux}} = \boldsymbol{U}'\boldsymbol{B}_{\text{aux}}\boldsymbol{T}_{\mathrm{i}} = \boldsymbol{U}'\bar{\boldsymbol{B}}\boldsymbol{T}_{\mathrm{i}} = \begin{bmatrix} 0 \\ 1 \end{bmatrix}$$

and partitioned accordingly

$$\tilde{\boldsymbol{A}}_{\text{aux}} = \boldsymbol{U}'\boldsymbol{A}_{\text{aux}}\boldsymbol{U} = \boldsymbol{U}'(\bar{\boldsymbol{A}} + \bar{\boldsymbol{B}}\boldsymbol{F})\boldsymbol{U} = \begin{bmatrix} \boldsymbol{A}_{11} & \boldsymbol{A}_{12} \\ \boldsymbol{A}_{21} & \boldsymbol{A}_{22} \end{bmatrix}$$

It was straightforward to verify that the stabilisability of $(\bar{\boldsymbol{A}}, \bar{\boldsymbol{B}})$ implies the stabilisability of $(\boldsymbol{A}_{11}, \boldsymbol{A}_{12})$. In fact, their uncontrollable modes, if any, are identical. Next, for determining an appropriate matrix $\boldsymbol{P} = \boldsymbol{P}' > 0$, we partitioned it accordingly as follows

$$\tilde{\boldsymbol{P}} = \boldsymbol{U}'\boldsymbol{P}\boldsymbol{U} = \begin{bmatrix} \boldsymbol{P}_{11} & \boldsymbol{P}_{21}' \\ \boldsymbol{P}_{21} & \boldsymbol{P}_{22} \end{bmatrix} \tag{54}$$

Then, $\boldsymbol{C}_{\text{aux}}$ can be expressed as

$$\begin{aligned} \boldsymbol{C}_{\text{aux}} &= \bar{\boldsymbol{B}}'\boldsymbol{P} = (\boldsymbol{T}_{\mathrm{i}}^{-1})'[0 \quad 1]\boldsymbol{U}'\boldsymbol{U}\begin{bmatrix} \boldsymbol{P}_{11} & \boldsymbol{P}_{21}' \\ \boldsymbol{P}_{21} & \boldsymbol{P}_{22} \end{bmatrix}\boldsymbol{U}' \\ &= (\boldsymbol{T}_{\mathrm{i}}^{-1})'[\boldsymbol{P}_{21} \ \boldsymbol{P}_{22}]\boldsymbol{U}' \\ &= [(\boldsymbol{T}_{\mathrm{i}}^{-1})' \ \boldsymbol{P}_{22}][\boldsymbol{P}_{22}^{-1}\boldsymbol{P}_{21} \quad 1]\boldsymbol{U}' \\ &:= \boldsymbol{T}_{\mathrm{o}}[\boldsymbol{P}_{22}^{-1}\boldsymbol{P}_{21} \ \ 1]\boldsymbol{U}' \end{aligned}$$

Using the results of Chen *et al.* [8] (see, for example, Chapters 8 and 9), we showed that the invariant zeros of the auxiliary system $\boldsymbol{G}_{\text{aux}}(z)$ were given by the eigenvalues of $\boldsymbol{A}_{11} - \boldsymbol{A}_{12}\boldsymbol{P}_{22}^{-1}\boldsymbol{P}_{21}$. As $(\boldsymbol{A}_{11}, \boldsymbol{A}_{12})$ was stabilisable and the given set of complex scalars included all its uncontrollable modes, there exists a constant matrix, say $\boldsymbol{F}_*$, such that $\boldsymbol{A}_{11} - \boldsymbol{A}_{12}\boldsymbol{F}_*$ has its eigenvalues placed exactly at the locations given in the set. Obviously, we can select $\boldsymbol{P}_{22}$ and $\boldsymbol{P}_{21}$ such that $\boldsymbol{P}_{22}^{-1}\boldsymbol{P}_{21} = \boldsymbol{F}_*$.

2. Selecting an appropriate $\boldsymbol{P}_{22} = \boldsymbol{P}_{22}' > 0$, $\boldsymbol{P}_{21} = \boldsymbol{P}_{22}\boldsymbol{F}_*$, and an appropriate $\boldsymbol{P}_{11} = \boldsymbol{P}_{11}' > \boldsymbol{P}_{21}'\boldsymbol{P}_{22}^{-1}\boldsymbol{P}_{21}$ ensures that

$$\boldsymbol{P} = \boldsymbol{U}\begin{bmatrix} \boldsymbol{P}_{11} & \boldsymbol{P}_{21}' \\ \boldsymbol{P}_{21} & \boldsymbol{P}_{22} \end{bmatrix}\boldsymbol{U}' > 0 \tag{55}$$

3. Compute

$$\boldsymbol{W} = \boldsymbol{P} - (\bar{\boldsymbol{A}} + \bar{\boldsymbol{B}}\boldsymbol{F})'\boldsymbol{P}(\bar{\boldsymbol{A}} + \bar{\boldsymbol{B}}\boldsymbol{F}) \tag{56}$$

If $\boldsymbol{W}$ is not a positive definite, go back to Step 2 and choose another solution of $\boldsymbol{P}$ or go to the first step to re-select another set of desired invariant zeros.

Another method for selecting $\boldsymbol{W}$ is based on a trial-and-error approach by limiting the choice of $\boldsymbol{W}$ to be in a diagonal matrix and adjusting its diagonal weights through simulation. Generally, such an approach would yield a satisfactory result as well.

2.4 Illustrative example

We illustrate the enhanced CNF control technique with the following example. We considered a discrete-time system of the form (1) with

$$\boldsymbol{A} = \begin{bmatrix} 0 & 1 & 0 \\ 0 & 0 & 1 \\ 1 & -3 & 3 \end{bmatrix}, \quad \boldsymbol{B} = \begin{bmatrix} 0 \\ 0 \\ 1 \end{bmatrix}$$

$$x_0 = \begin{pmatrix} 0 \\ 0 \\ 0.5 \end{pmatrix}, \quad \boldsymbol{E} = \begin{bmatrix} 1 \\ 0 \\ 1 \end{bmatrix}$$

$$\boldsymbol{C}_1 = \boldsymbol{I}_3, \quad \boldsymbol{C}_2 = [1 \quad 0 \quad 0]$$

and $u_{\max} = 1$. The disturbance w is unknown. For simulation purposes, we assume $w = -0.1$. Our goal was to design a CNF state feedback control law that would yield a good transient performance in tracking a target reference $r = 2$.

Following the procedure given in the previous section, to obtain an appropriate augmented system, an integration gain $\kappa_{\mathrm{i}} = 0.3$ was selected. After a few tries, we found that the following state feedback gain to the augmented system would yield a good performance for our problem

$$\boldsymbol{F} = [-0.1 \quad -0.85 \quad 2.14 \quad -1.7] \tag{57}$$

This placed the poles of $\bar{\boldsymbol{A}} + \bar{\boldsymbol{B}}\boldsymbol{F}$ at 0.9, 0.4, $0.5 \pm j0.5$. Note that the first one corresponds to the integrator. Both the linear state feedback control and enhanced CNF control share the same integration dynamics:

$$x_{\mathrm{i}}(k+1) = x_{\mathrm{i}}(k) + 0.3[h(k) - r] \tag{58}$$

The linear state feedback control law is given by

$$u(k) = [-0.85 \quad 2.14 \quad -1.7]x(k) - 0.1x_{\mathrm{i}}(k) + 0.41r \tag{59}$$

Letting $\boldsymbol{W} = \operatorname{diag}\{0.1, 1, 1, 1\}$, a positive definite solution $\boldsymbol{P}$ for (10) is obtained, which is given by

$$\boldsymbol{P} = \begin{bmatrix} 2.6201 & 0.7258 & 0.6543 & 1.1678 \\ 0.7258 & 1.6414 & -1.4825 & 2.1586 \\ 0.6543 & -1.4825 & 8.8061 & -7.3158 \\ 1.1678 & 2.1586 & -7.3158 & 13.3551 \end{bmatrix} \tag{60}$$

and a CNF state feedback law

$$\begin{aligned} u(k) &= [-0.85 \quad 2.14 \quad -1.7]x(k) - 0.1x_{\mathrm{i}}(k) + 0.41r \\ &\quad + \boldsymbol{\rho}(e(k))[-0.1678 \quad 2.3536 \quad -9.3268 \quad 10.0458] \\ &\quad \times \left[\begin{pmatrix} x_{\mathrm{i}}(k) \\ x(k) \end{pmatrix} - \begin{pmatrix} 0 \\ 2 \\ 2 \\ 2 \end{pmatrix} \right] \end{aligned} \tag{61}$$

where $\boldsymbol{\rho}$ is as given in (50) with $\alpha = 20$ and $\beta = 1.5$. The simulation results given in Figs. 1 and 2 clearly show that the CNF control has outperformed the linear control.

3 Design of a micro hard disk drive servo system

In this section, we apply the proposed technique given in the previous section to design a servo system for an IBM microdrive (DMDM-10340). The dynamic model of the voice-coil-motor (VCM) actuator of the microdrive has been fully identified in Peng *et al.* [7] and is given by

$$y = \boldsymbol{G}(s)(u + w) \tag{62}$$

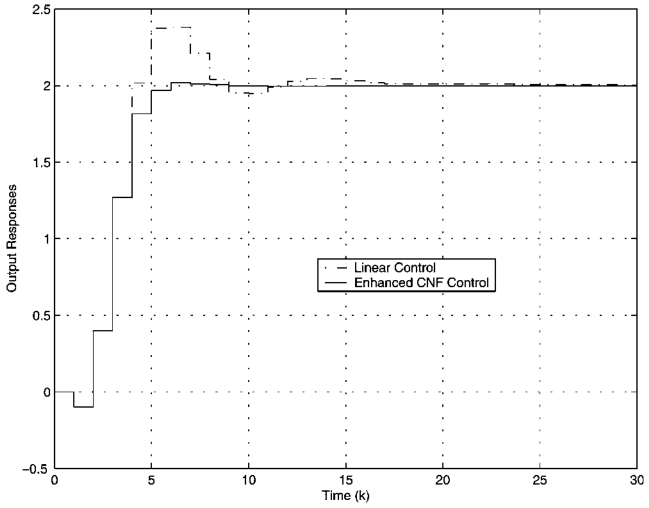

Fig. 1 *Output responses of the enhanced CNF control and linear control*

where y is in μm, the relative displacement of the read/write (R/W) head, u, is in Volts, the input signal to the VCM actuator, which has a saturation level $u_{\max} = 3$ V and w is the input disturbances including friction and bias torque, which is around -0.008 V. The transfer function $\boldsymbol{G}(s)$ is given as

$$\boldsymbol{G}(s) = \frac{2.35 \times 10^8}{s^2} \boldsymbol{G}_{\text{r.m.}}(s) \tag{63}$$

where

$$\begin{aligned} \boldsymbol{G}_{\text{r.m.}}(s) = & \frac{0.8709s^2 + 1726s + 1.369 \times 10^9}{s^2 + 1480s + 1.369 \times 10^9} \\ & \times \frac{0.9332s^2 - 805.8s + 1.739 \times 10^9}{s^2 + 125.1s + 1.739 \times 10^9} \\ & \times \frac{1.072s^2 + 925.1s + 1.997 \times 10^9}{s^2 + 536.2s + 1.997 \times 10^9} \\ & \times \frac{0.9594s^2 + 98.22s + 2.514 \times 10^9}{s^2 + 1805s + 2.514 \times 10^9} \\ & \times \frac{7.877 \times 10^9}{s^2 + 6212s + 7.877 \times 10^9} \end{aligned} \tag{64}$$

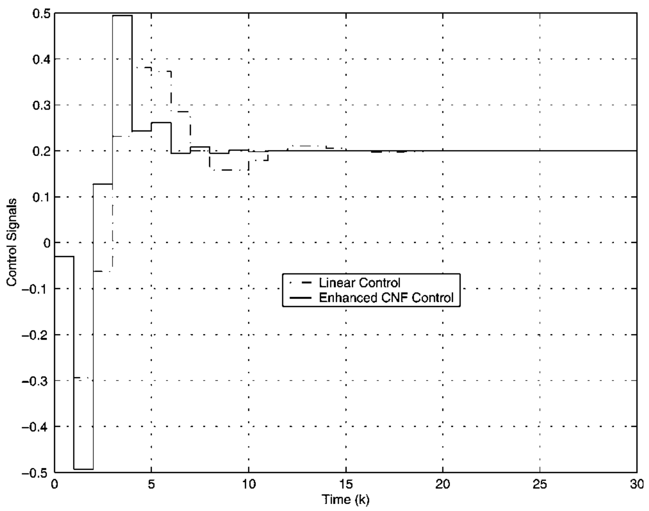

Fig. 2 *Control signals of the enhanced CNF control and linear control*

represents the resonant modes of the VCM actuator of the microdrive. The transfer function is identified by matching the measured frequency response (Fig. 3). The discretised counterpart of the simplified (nominal) model of the HDD system is given by

$$x(k+1) = \begin{bmatrix} 1 & T \\ 0 & 1 \end{bmatrix} x(k) + \begin{bmatrix} 0.5aT^2 \\ aT \end{bmatrix} [\text{sat}(u(k)) + w] \tag{65}$$

and

$$y(k) = h(k) = [1 \quad 0] x(k) \tag{66}$$

where $T = 10^{-4}$ s is the sampling period and $a = 2.35 \times 10^8$. The initial state was assumed to be $x(0) = 0$. The task was to design a track following controller for the drive using the proposed technique. More specifically, the aim was to design a controller that was capable of moving the actuator to a target track as fast as possible with limited control amplitude, and maintaining the tip of the actuator, that is, the R/W head, as close as possible to the track centre while data was being read or written. A target reference $r = 1$ was the focus of the design, which corresponds to one or two tracks for a disk drive with a track density of 40 000 tracks per inch (TPI). The design specifications were: (1) that the control signal did not exceed the saturation level; (2) that the gain margin was not less than 6 dB and the phase margin was not less than 45° (equivalent to about 60° in the continuous-time domain, if we considered the phase lag caused by the zero-order hold in discrete domain); and (3) that there was no steady state bias and fast settling time. Here settling time is defined as the time it takes for the R/W head to reach and remain in the 0.03 μm neighbourhood of the target track.

Following the procedure given in Section 2, an integration term is introduced

$$x_i(k+1) = x_i(k) + [h(k) - r] \tag{67}$$

The corresponding augmented plant is then given by

$$\begin{cases} \bar{x}(k+1) = \begin{bmatrix} 1 & 1 & 0 \\ 0 & 1 & T \\ 0 & 0 & 1 \end{bmatrix} \bar{x}(k) + \begin{bmatrix} -1 \\ 0 \\ 0 \end{bmatrix} r \\ \qquad + \begin{bmatrix} 0 \\ 0.5aT^2 \\ aT \end{bmatrix} \text{sat}[u(k)] + \begin{bmatrix} 0 \\ 0.5aT^2 \\ aT \end{bmatrix} w \\ \bar{y}(k) = \begin{bmatrix} 1 & 0 & 0 \\ 0 & 1 & 0 \end{bmatrix} \bar{x}(k) \\ h(k) = [0 \quad 1 \quad 0] \bar{x}(k) \end{cases} \tag{68}$$

For the above augmented system, a state feedback gain matrix

$$\boldsymbol{F} = -[1.7911 \times 10^{-5} \quad 0.0598 \quad 1.4857 \times 10^{-5}] \tag{69}$$

was designed which placed the poles of $\bar{\boldsymbol{A}} + \bar{\boldsymbol{B}}\boldsymbol{F}$ at 0.9997 and $0.7905 \pm j0.3105$. Note that the conjugate pair have a damping ratio of 0.4 and a natural frequency of 650 Hz, which is the working frequency of the actuator. Next, a reduced-order observer gain matrix $\boldsymbol{K}_{\text{R}} = -4511.9$ to place the observer pole at 0.5488 was designed, and the matrix $\boldsymbol{W} = \text{diag}\{1.1 \times 10^{-6},\ 0.01,\ 2.6 \times 10^{-9}\}$ was chosen, which lead to a reduced-order CNF controller

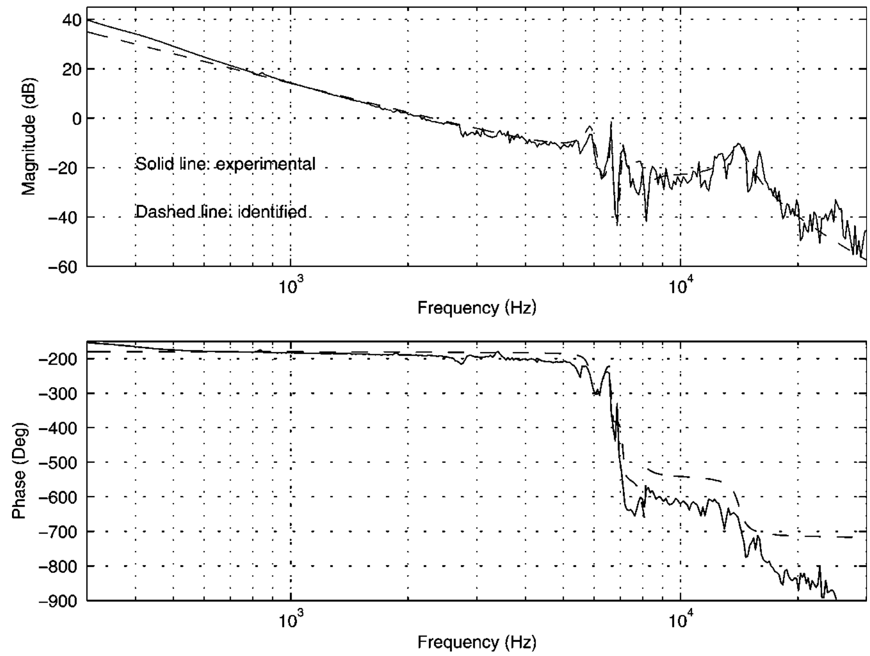

Fig. 3 *Frequency response of the IBM microdrive*

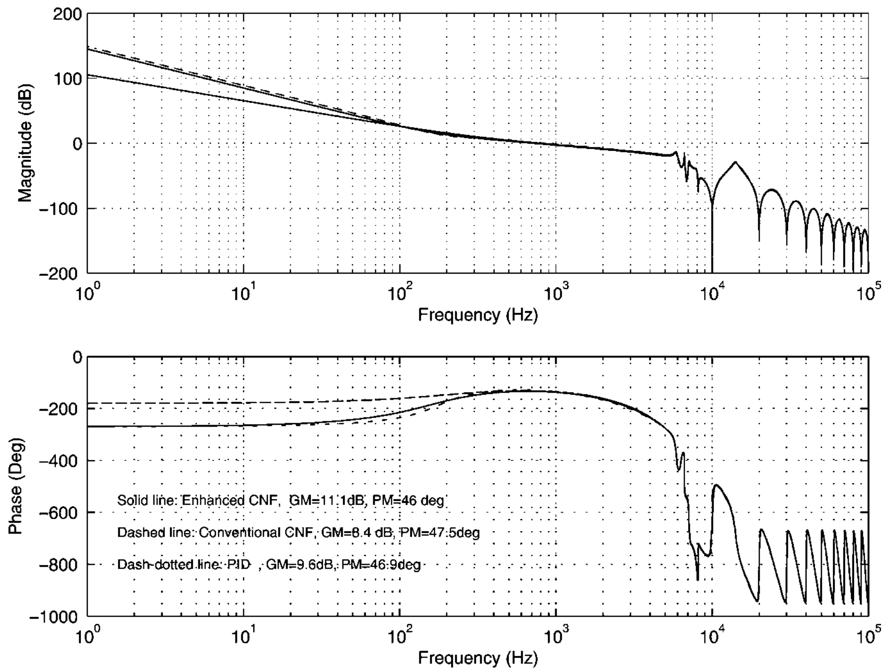

Fig. 4 *Open-loop frequency response of the HDD servo systems*

characterised by

$$\begin{pmatrix} x_i(k+1) \\ x_v(k+1) \end{pmatrix} = \begin{bmatrix} 1 & 0 \\ 0 & 0.5488 \end{bmatrix} \begin{pmatrix} x_i(k) \\ x_v(k) \end{pmatrix} - \begin{bmatrix} 1 \\ 0 \end{bmatrix} r + \begin{bmatrix} 0 \\ 18199 \end{bmatrix} \mathrm{sat}(u(k)) + \begin{bmatrix} 1 \\ -2035.7 \end{bmatrix} y(k) \tag{70}$$

and

$$u(k) = (\boldsymbol{\rho}(e(k))[\,0.0307 \quad 0.0462 \quad 1.3398 \times 10^{-4}\,] - [\,1.7911 \times 10^{-5} \quad 0.0598 \quad 1.4857 \times 10^{-5}\,])x_r(k) \tag{71}$$

where

$$x_r(k) = \begin{pmatrix} x_i(k) \\ y(k) - r \\ x_v(k) + 4511.9y(k) \end{pmatrix} \tag{72}$$

Table 1: Stability margins of the HDD servo systems

Controller	Classical PID	Conventional CNF	Enhanced CNF
Gain margin (dB)	9.6	8.4	11.1
Phase margin (°)	46.9	47.5	46

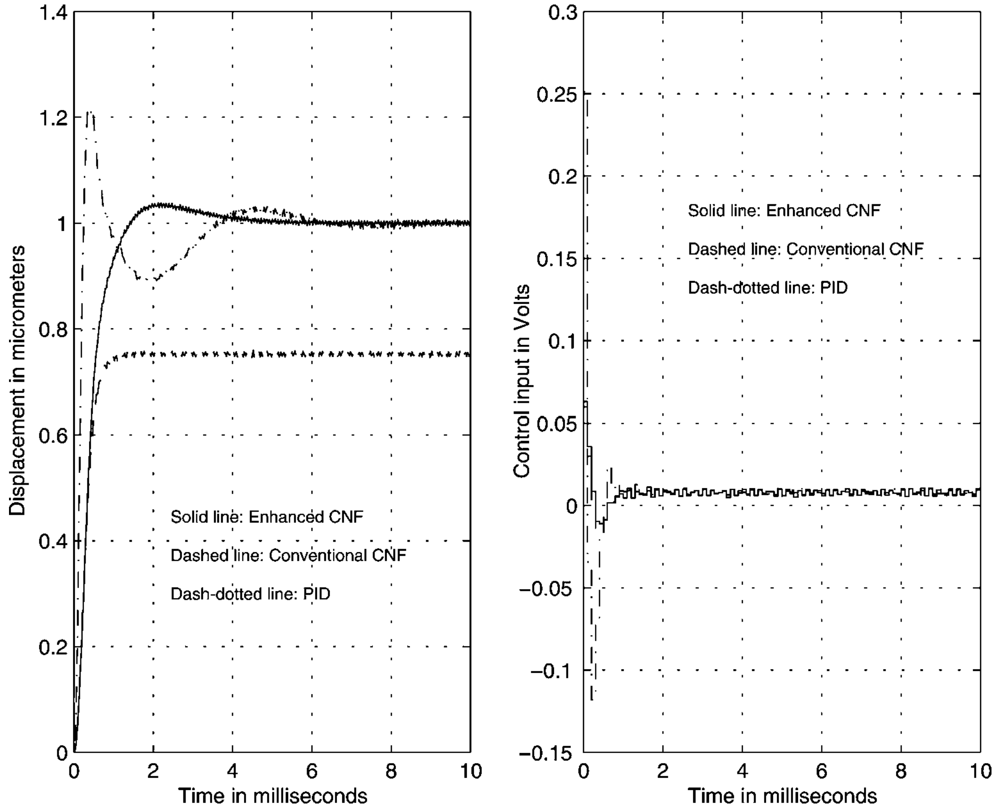

Fig. 5 *Simulation results of the HDD servo systems*

and the nonlinear gain function was selected as

$$\rho(e(k)) = -0.191 \arctan\left(\Big||e(k)| - |h(0) - r|\Big|\right) \quad (73)$$

For comparison, a conventional reduced-order CNF controller without integration using the method reported in Venkataramanan *et al.* [6] was designed and is characterised by

$$x_v(k+1) = 0.5488 x_v(k) - 2035.7 y(k) + 1.8199 \times 10^4 \, \mathrm{sat}(u(k)) \quad (74)$$

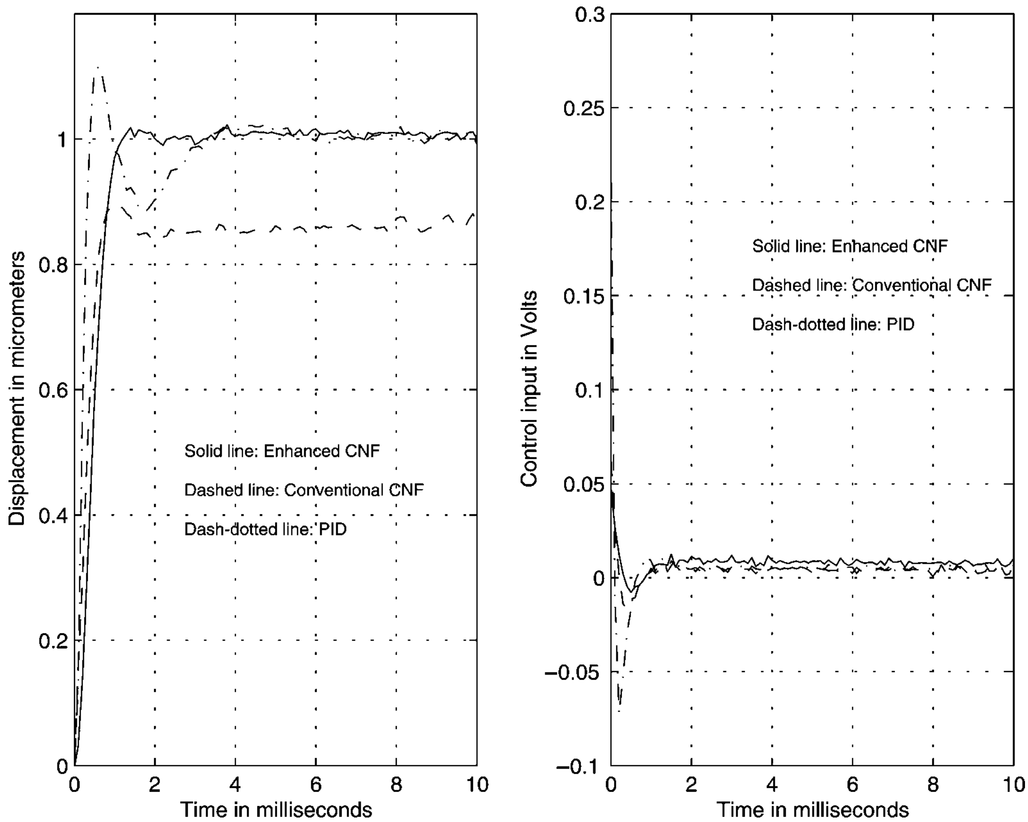

Fig. 6 *Experimental results of the HDD servo systems*

Table 2: Settling time (ms): enhanced CNF against PID

	Classical PID	Enhanced CNF	Improvement (%)
Simulation	4.5	1.2	73
Implementation	2.8	1.1	61

and

$$u(k) = (\tilde{\rho}(e(k))[\,0.0372 \quad 3.5584 \times 10^{-5}\,] \\ -[\,0.0629 \quad 2.0598 \times 10^{-5}\,])\begin{pmatrix} y(k) - r \\ x_v(k) + 4511.9y(k) \end{pmatrix} \tag{75}$$

where

$$\tilde{\rho}(e(k)) = -0.6366 \arctan\left(\left||e(k)| - |h(0) - r|\right|\right) \tag{76}$$

We also compared the servo performance of the above design with a best-tuned PID controller

$$u(k) = \left(k_p + \frac{k_d(z-1)}{Tz} + \frac{k_i Tz}{z-1}\right)[r - y(k)] \tag{77}$$

where $T = 10^{-4}$ s is the sampling period, $k_p = 0.023$, $k_d = 2.2512 \times 10^{-5}$ and $k_i = 30$.

The gain margin and phase margin for the conventional CNF and the enhanced CNF control were computed at steady state when $\rho(e(k))$ or $\tilde{\rho}(e(k))$ converged to a constant. Fig. 4 shows the frequency domain properties of the designed servo systems. The resulting gain and phase margins are listed in Table 1, which clearly indicate that all the designed controllers satisfy the design specifications.

For simulation, we used the actuator model given in (62), which includes all its resonance modes. The simulations were done in a mix setting where the plant was in continuous-time and the controller was in discrete-time with a zero-order hold operator being utilised. For experiment, we used an actual IBM microdrive with its cover removed. The only measurable output is the relative displacement of the R/W head and was measured by a laser Doppler vibrometer. The controllers were implemented with a sampling frequency of 10 kHz on a dSpace DSP board installed on a personal computer.

The simulation and experimental results are respectively shown in Figs. 5 and 6. Clearly, the conventional CNF controller failed to bring the R/W head into the desired target neighbourhood and the PID controller resulted in a large overshoot and undershoot. The enhanced CNF controller was able to move the R/W head to the target fast and smoothly. The tracking performances (in terms of settling time) are summarised in Table 2. Obviously, the performance of the enhanced CNF control is much better than that of the PID control. It effectively removes the steady-state bias without sacrificing transient performance.

4 Concluding remarks

We have presented a nonlinear control technique, that is, enhanced CNF control, for a class of discrete-time systems with input saturation and with unknown disturbances. The new technique is capable of yielding better performance (i.e. faster settling time and smaller overshoot) compared with that of linear control. The enhanced CNF control is also capable of eliminating steady-state bias because of the disturbances. A numerical example and a practical design of a disk drive servo system have been provided to demonstrate the effectiveness of this control technique. The result can be generalised to more general discrete-time MIMO systems.

5 References

1 Dorf, R.C.: 'Modern control systems' (Addison Wesley, Massachusetts, 1992, 7th edn.)
2 Huang, J.: 'Nonlinear output regulation: theory and applications' (SIAM, Philadelphia, 2004)
3 Lin, Z., Pachter, M., and Banda, S.: 'Toward improvement of tracking performance—nonlinear feedback for linear systems', *Int. J. Control*, 1998, **70**, (1), pp. 1–11
4 Turner, M.C., Postlethwaite, I., and Walker, D.J.: 'Nonlinear tracking control for multivariable constrained input linear systems', *Int. J. Control*, 2000, **73**, (12), pp. 1160–1172
5 Chen, B.M., Lee, T.H., Peng, K., and Venkataramanan, V.: 'Composite nonlinear feedback control: theory and an application', *IEEE Trans. Automat. Control*, 2003, **48**, (3), pp. 427–439
6 Venkataramanan, V., Peng, K., Chen, B.M., and Lee, T.H.: 'Discrete-time composite nonlinear feedback control with an application in design of a hard disk drive servo system', *IEEE Trans. Control Syst. Technol.*, 2003, **11**, (1), pp. 16–23
7 Peng, K., Chen, B.M., Cheng, G., and Lee, T.H.: 'Modeling and compensation of nonlinearities and friction in a micro hard disk drive servo system with nonlinear feedback control', *IEEE Trans. Control Syst. Technol.*, 2005, **13**, (5), pp. 708–721
8 Chen, B.M., Lin, Z., and Shamash, Y.: 'Linear systems theory: a structural decomposition approach' (Birkhauser, Boston, 2004)